Author Manuscript

Author Manuscript

Author Manuscript

Author Manuscript

HHS Public Access

Author manuscript

Nat Struct Mol Biol. Author manuscript; available in PMC 2016 June 06.

Published in final edited form as:

Nat Struct Mol Biol. 2007 October ; 14(10): 949–958. doi:10.1038/nsmb1292.

Distinct domains of Complexin I differentially regulate neurotransmitter release

Mingshan Xue[1,2,6], **Kerstin Reim**[3,6], **Xiaocheng Chen**[4,5], **Hsiao-Tuan Chao**[1,2], **Hui Deng**[1,2], **Josep Rizo**[4,5], **Nils Brose**[3,7], and **Christian Rosenmund**[1,2,7]

[1]Department of Neuroscience, Baylor College of Medicine, Houston, Texas 77030, USA

[2]Department of Molecular and Human Genetics, Baylor College of Medicine, Houston, Texas 77030, USA

[3]Department of Molecular Neurobiology, Max Planck Institute of Experimental Medicine, D-37075 Göttingen, Germany

[4]Department of Biochemistry, University of Texas Southwestern Medical Center, Dallas, Texas 75390, USA

[5]Department of Pharmacology, University of Texas Southwestern Medical Center, Dallas, Texas 75390, USA

Abstract

Complexins constitute a family of four synaptic high-affinity SNARE complex binding proteins. They positively regulate a late, post-priming step in Ca^{2+}-triggered synchronous neurotransmitter release, but the underlying molecular mechanisms are unclear. We show here that SNARE complex binding of Complexin I via its central α-helix is necessary but unexpectedly not sufficient for its key function in promoting neurotransmitter release. An accessory α-helix N-terminal of the SNARE complex binding region plays an inhibitory role in fast synaptic exocytosis, while its N-terminally adjacent sequences facilitate Ca^{2+}-triggered release even in the absence of the Ca^{2+} sensor Synaptotagmin 1. Our results indicate that distinct functional domains of Complexins differentially regulate synaptic exocytosis, and that via the interplay between these domains Complexins play a crucial role in fine-tuning Ca^{2+}-triggered fast neurotransmitter release.

Introduction

The precise timing of neurotransmitter release is crucial for information processing in the nervous system. To achieve this exquisite regulation, release is controlled by a complex protein apparatus. Central components of this machinery are the soluble N-ethylmaleimide-sensitive factor attachment protein receptors (SNAREs), Synaptobrevin 2, Syntaxin 1 and SNAP-25, which belong to a conserved family of membrane-associated proteins with a

Users may view, print, copy, download and text and data- mine the content in such documents, for the purposes of academic research, subject always to the full Conditions of use: http://www.nature.com/authors/editorial_policies/license.html#terms

[7]To whom correspondence should be addressed: ; Email: brose@em.mpg.de (N.B.) or ; Email: rosenmun@bcm.tmc.edu (C.R.)
[6]These authors contributed equally to this work.

Competing Interests Statement: The authors declare no competing financial interests.

Author Manuscript Author Manuscript Author Manuscript Author Manuscript

central role in membrane fusion[1]. The SNAREs form a tight four-helix bundle, the SNARE complex, through the sequences called SNARE motifs[2,3]. SNARE complex formation brings the vesicle and plasma membrane into close apposition, which is likely essential for membrane fusion[1,4]. Among additional factors that are required to accomplish the extreme speed and exquisite Ca^{2+}-sensitivity of vesicle fusion at synapses, Synaptotagmin 1 (Syt1), which acts as a Ca^{2+} sensor[5], and Complexins (Cplxs, also called Synaphins) are particularly important.

Complexins are encoded by four genes (*Cplx*I-IV) and constitute a family of small (15-18 kDa), acidic proteins[6-9]. Cplxs bind to the assembled SNARE complex, but not to individual SNAREs, through a central α-helix that interacts with the SNARE motifs of Syntaxin 1 and Synaptobrevin 2[8,10-15]. In addition, Cplxs contain an accessory α-helix that does not contact the SNARE complex[12], and additional N- and C-terminal sequences with unknown function.

Studies on CplxI and II double knockout (CplxI/II DKO) mice indicated that CplxI and II are crucial positive regulators of synaptic vesicle exocytosis *in vivo* and act at or following the Ca^{2+} triggering step of neurotransmitter release[16]. Cross rescue experiments showed that CplxIII and IV can functionally replace CplxI and II in hippocampal neurons, indicating that CplxIII and IV also act as positive regulators of neurotransmitter release[9]. Several studies confirmed that Cplxs promote transmitter release[17,18], but others indicated an inhibitory function for Cplxs[19,20]. Recent reports using reconstituted liposome and cell fusion assays indicated that Cplxs act as “clamps” of SNARE-mediated membrane fusion, which is released by Ca^{2+}-bound Syt1[21,22]. Another observation also indicated an inhibitory role for Cplxs in release by showing that fusing CplxI to Synaptobrevin 2 outcompetes Syt1 for SNARE complex binding and abrogates Ca^{2+}-triggered synchronous release[23]. These studies also indicate that Cplxs and Syt1 may be functionally coupled. Furthermore, deletion of Syt1 abolishes synchronous release while asynchronous release remains intact, which is similar to but more severe than the CplxI/II DKO phenotype[24,25]. Therefore, it was proposed that Cplxs fully assemble the SNARE complex and transform vesicles into a metastable state that serves as the substrate for Syt1 to trigger fast release[12,23,26].

Clearly, Cplxs play a crucial role in regulating synaptic exocytosis, but the precise molecular mechanism and the structural basis of Cplxs function remain unclear. To shed light on these questions, we performed a detailed quantitative structure-function analysis of CplxI function in mouse hippocampal glutamatergic synapses. Our data showed that binding of the central α-helix to the SNARE complex is essential for CplxI function, providing at the same time strong evidence for the physiological importance of the SNARE complex itself in neurotransmitter release. Furthermore, we found that the accessory α-helix of CplxI plays an inhibitory role in release, while the first 26 residues of CplxI have a crucial active function that may be associated to a novel interaction. The dual functions of the N terminus of CplxI require the SNARE complex binding. These results show that different domains of CplxI have distinct functions in promoting or inhibiting Ca^{2+}-triggered release, indicating that an intricate interplay between these domains plays a crucial role in fine-tuning the speed and the Ca^{2+}-sensitivity of neurotransmitter release.

Author Manuscript Author Manuscript Author Manuscript Author Manuscript

Results

Overexpression of CplxI rescues CplxI/II DKO

CplxI/II DKO hippocampal glutamatergic neurons show reduced vesicular release probability (P_{vr}), increased paired-pulse ratio and decreased Ca^{2+}-sensitivity of synchronous release[16]. For a systematic structure-function analysis of CplxI, we utilized a KO-rescue approach and used these three synaptic characteristics (see METHODS) as readouts for CplxI function. We first compared CplxII KO neurons (indistinguishable from WT neurons[16]), CplxI/II DKO neurons and CplxI/II DKO neurons overexpressing WT CplxI by Semliki-Forest virus (SFV)[27] (Fig. 1).

Action potential evoked excitatory postsynaptic current (EPSC) amplitudes were reduced by 58% in CplxI/II DKO neurons and restored to control levels after overexpression of WT CplxI (Fig. 1a,e). The sizes of the readily releasable pool of vesicles (RRP) measured by hypertonic solution[28] were not significantly different among the three groups ($p = 0.7$, Fig. 1b,f). Consequently, P_{vr} was reduced by 46% in CplxI/II DKO neurons, while the P_{vr} of CplxI/II DKO neurons rescued with WT CplxI was indistinguishable from that of control neurons (Fig. 1g). The altered synaptic short-term plasticity of CplxI/II DKO neurons as measured by 5 EPSCs at 50 Hz (i.e., 20 ms inter-stimulus interval, ISI) was converted to WT characteristics upon overexpression of WT CplxI (Fig. 1c,h). The right-shift of the apparent Ca^{2+}-sensitivity of synchronous release in CplxI/II DKO neurons was also restored by overexpression of WT CplxI. The degrees of EPSC amplitude potentiation and depression upon switching from standard Ca^{2+} concentrations (4 mM Ca^{2+}/4 mM Mg^{2+}) to high Ca^{2+} concentrations (12 mM Ca^{2+}/1 mM Mg^{2+}) and low Ca^{2+}-concentrations (1 mM Ca^{2+}/1 mM Mg^{2+}) were similar between the rescue and control groups (Fig. 1d,i,j).

Taken together, the above data show that the temporary lack of CplxI and II does not cause irreversible effects on synaptic function, and that overexpression of WT CplxI can fully reconstitute WT-like synaptic function in CplxI/II DKO neurons.

Synaptic function is not sensitive to Cplx levels

The fusion clamp model of Cplxs predicts that elevated Cplx levels may inhibit neurotransmitter release[21,22]. Moreover, CplxII is down-regulated in several neurological disorders, including a transgenic mouse model of Huntington's disease[29]. We therefore examined how sensitive synaptic function is to altered Cplx levels in our genetically well-characterized system.

We studied neurons lacking CplxII and containing only one functional CplxI allele (CplxI Het/CplxII KO) to test the sensitivity of synaptic function to strong reduction in Cplx levels. We also examined whether a more than 10-fold overexpression of CplxI (Supplementary Fig. 1a online) changed synaptic function in WT neurons. We found that neither of these two manipulations altered synaptic transmission, as evoked EPSC amplitude, RRP size, P_{vr}, paired-pulse ratio, and Ca^{2+}-sensitivity were not significantly changed ($p > 0.05$ for all tested parameters, Fig. 2a-d; data not shown). Thus, at hippocampal glutamatergic synapses, transmitter release is not sensitive to either severe reduction or strong elevation of Cplx levels. CplxI and II have a steady positive effect on Ca^{2+}-triggered neurotransmitter release

Author Manuscript Author Manuscript Author Manuscript Author Manuscript

over a wide range of expression levels. Hence, Cplxs do not act merely as fusion clamps in synaptic exocytosis.

Mutations in CplxI that block SNARE complex binding

In order to test the functional significance of Cplxs binding to the SNARE complex, we identified CplxI mutants with deficient SNARE complex binding by an initial random mutagenesis approach[30] and a site-directed mutagenesis approach based on the structure of the CplxI-SNARE complex[12,13]. In the random mutagenesis experiments, we generated 20 independent full-length CplxI clones with missense mutations in CplxI (Fig. 3a). Glutathione S-transferase (GST) tagged CplxI WT and mutants were tested for the binding to the SNARE complex in cosedimentation assays. None of the missense mutations outside of the previously defined SNARE complex binding region (48-70 of CplxI[12]) influenced the interaction with the neuronal SNARE complex (Fig. 3a-c; data not shown). Three single mutations (R48L, R59H, G71D) perturbed SNARE complex binding and the double mutations (R48L R59H) abolished the binding (Fig. 3b-d).

The structure of the CplxI-SNARE complex indicates that two tyrosine (Tyr52, Tyr70), three arginine (Arg48, Arg59, Arg63), and one lysine (Lys69) residues of CplxI are critical for the binding to the SNARE complex[12]. We mutated these residues (Y52A, R63A, K69A Y70A) and found that SNARE complex binding was either strongly reduced (Y52A) or abolished (R63A, K69A Y70A; Fig. 3d). Together, these data verify the predictions of the structural studies and demonstrate that individual amino acids in the central part of CplxI are essential for SNARE complex binding.

SNARE complex binding is necessary for CplxI function

To investigate the functional relevance of CplxI binding to the SNARE complex *in vivo*, we examined the rescue activities of SNARE complex binding deficient CplxI mutants in CplxI/II DKO neurons. In this series of experiments, we compared CplxI/II DKO neurons rescued with CplxI mutants to those rescued with WT CplxI . The expression levels of all tested CplxI mutants in neurons were 8-13 times higher than the endogenous CplxI levels (Supplementary Fig. 1 online), and they were all properly targeted to the presynaptic terminals (Supplementary Fig. 2 online). We normalized the data to the mean values of the corresponding WT CplxI rescue to allow for comparison of different CplxI mutants across different experiments. To better assess intermediate phenotypes associated with partial loss-of-function CplxI mutants, we often included CplxI/II DKO neurons rescued with EGFP only as negative controls. We pooled all the data from CplxI/II DKO neurons during the entire study in Figures 4 and 5 as the normalized CplxI/II DKO values did not vary significantly across different experiments and cultures ($p > 0.05$ for all groups).

We first examined P_{vr} and paired-pulse ratio. Overexpression of WT CplxI fully rescued the reduced P_{vr} and increased paired-pulse ratio in CplxI/II DKO neurons (Figs. 1 and 4). Comparable full rescue activity was obtained with D29V mutant (Fig. 4c,d), which bound to the SNARE complex normally (Fig. 3b,c). R59H mutant showed reduced SNARE binding activity (Fig. 3b,c), and CplxI/II DKO neurons rescued with this mutant exhibited decreased release, which indicated a partial loss-of-function for R59H (Fig. 4c,d). Release was further

Author Manuscript Author Manuscript Author Manuscript Author Manuscript

reduced in CplxI/II DKO neurons rescued with the double mutant R48L R59H (Fig. 4c,d). The double mutant K69A Y70A, which completely lacks SNARE complex binding (Fig. 3d), had almost no rescue activity because the P_{vr} and paired-pulse ratio did not differ significantly from those of CplxI/II DKO neurons ($p = 0.8$ and $p = 0.5$, respectively, Fig. 4c,d). A similar rescue pattern was seen when we assayed the Ca^{2+}-sensitivity of synchronous release (Fig. 4b,e,f).

The strong correlations between our biochemical and electrophysiological data provide the *in vivo* evidence that the SNARE complex interaction of CplxI is essential for its key role in regulating fast neurotransmitter release, and that the SNARE complex itself plays an important role in this process.

SNARE complex binding is not sufficient for CplxI function

To examine whether SNARE complex binding is sufficient for CplxI function or whether the N- and C-terminal sequences outside the central α-helix contribute to CplxI function, we generated a CplxI deletion mutant, $CplxI_{47–75}$, containing only the minimal SNARE complex binding region (Fig. 5a). When we rescued CplxI/II DKO neurons with this CplxI fragment, we found strongly impaired rescue activity (Supplementary Fig. 3 online), but $CplxI_{47–75}$ also showed reduced binding to the SNARE complex (Fig. 5b), which complicated the interpretation of the reduced rescue activity of $CplxI_{47–75}$. Therefore, we generated CplxI truncation mutants lacking either the N terminus ($CplxI_{47–134}$) or the C terminus ($CplxI_{1–75}$). $CplxI_{1–75}$ bound normally to the SNARE complex, while the binding of $CplxI_{47–134}$ was only slightly reduced (Fig. 5b). We found that $CplxI_{1–75}$ had normal rescue efficacy (data not shown), and $CplxI_{47–134}$ showed an impaired rescue activity as compared to CplxI WT (Fig. 5c-f, Supplementary Fig. 3 online). These results indicate that the SNARE complex interaction is necessary but not sufficient for CplxI function.

Dual roles of CplxI N terminus in transmitter release

To dissect the regulatory function of the N-terminal domains of CplxI, we generated a CplxI N-terminal truncation mutant that lacks the first 26 residues but includes the accessory α-helix, $CplxI_{27–134}$ (Fig. 5a). This mutant bound to the SNARE complex normally (Fig. 5b). Surprisingly, we found a complete loss-of-function phenotype when we rescued CplxI/II DKO neurons with $CplxI_{27–134}$, a phenotype that was much more severe than $CplxI_{47–134}$. The P_{vr} (Fig. 5c) and paired-pulse ratio (Fig. 5d) were 55% and 162% of control values, respectively, and did not differ significantly from those of CplxI/II DKO neurons ($p = 0.4$ and $p = 0.8$, respectively). The Ca^{2+}-sensitivity was also similar to that of CplxI/II DKO neurons ($p = 0.8$ for 12 mM Ca^{2+} potentiation and $p = 0.4$ for 1 mM Ca^{2+} depression; Fig. 5e,f).

$CplxI_{47–134}$ rescue experiments indicate that the N-terminal domains of CplxI play a modulatory role in CplxI function. Contrary to expectation, the results of $CplxI_{27–134}$ imply that the first 26 residues of CplxI are essential for its function. Western blotting and immunocytochemistry revealed that sufficient amounts of $CplxI_{27–134}$ were expressed in neurons and targeted to the presynaptic terminals (Supplementary Figs. 1 and 2 online). The SNARE complex binding of $CplxI_{27–134}$ was also normal (Fig. 5b). Our results indicate that

Author Manuscript Author Manuscript Author Manuscript Author Manuscript

the central α-helix, the accessory α-helix, and the very N terminus (residues 1-26) of CplxI play distinct roles in regulating neurotransmitter release. The central α-helix of CplxI binds to the SNARE complex to promote release. The accessory α-helix (residues 29-47) has a negative regulatory effect on vesicle fusion, while the first 26 residues have a strong facilitating function. In this scenario, the N-terminal deletion mutant $CplxI_{47–134}$ loses both the positive function of the first 26 residues, and the negative function of the accessory α-helix. Therefore, it may show a better rescue activity than $CplxI_{27–134}$ in CplxI/II DKO neurons. Indeed, all tested synaptic parameters of CplxI/II DKO neurons rescued with $CplxI_{47–134}$ were significantly different from those of CplxI/II DKO neurons rescued with $CplxI_{27–134}$ ($p < 0.001$ for all of P_{vr}, paired-pulse ratio and Ca^{2+}-sensitivity; Fig. 5c-f). These results also confirm that the SNARE complex binding is not sufficient for CplxI function and the N-terminal sequences contribute to its function.

Inhibitory function of the accessory α-helix of CplxI

Our results demonstrate an overall positive role of CplxI in promoting synaptic vesicle fusion, while the accessory α-helix exerts an inhibitory effect on Ca^{2+}-triggered release. To gain insight into the molecular mechanism underlying the inhibitory function of the accessory α-helix, we generated a CplxI mutant ($CplxI_{41–134}$) with the accessory α-helix partially truncated (Fig. 5a). $CplxI_{41–134}$ bound to the SNARE complex like WT (Fig. 5b). In the rescue experiments with CplxI/II DKO neurons, $CplxI_{41–134}$ exhibited a partial loss-of-function phenotype (Fig. 5c-f), similar to $CplxI_{47–134}$ that lacks the entire accessory α-helix. Furthermore, $CplxI_{41–134}$, like $CplxI_{47–134}$, showed enhanced rescue activity as compared to $CplxI_{27–134}$ ($p < 0.01$ for all of P_{vr}, paired-pulse ratio and Ca^{2+}-sensitivity, Fig. 5c-f). Thus, the inhibitory function of the accessory α-helix requires the complete accessory α-helical structure.

To examine whether the inhibitory function of the accessory α-helix is dependent on its α-helical conformation, we generated a mutant carrying a helix-breaking mutation in this region (L41P). To verify the effect of this mutation, we generated a recombinant CplxI comprising residues 26-83 with the L41P mutation ($CplxI_{26–83}$ L41P), and acquired a series of NMR spectra of $CplxI_{26–83}$ L41P in isolation or bound to the SNARE complex. The structural data indicated that the L41P mutation caused little changes on the SNARE complex binding mode of CplxI, but strongly perturbed the accessory α-helix (see Supplementary Data and Supplementary Fig. 4 online).

When we rescued CplxI/II DKO neurons with $CplxI_{27–134}$ L41P, we found similar effects to those of $CplxI_{41–134}$ and $CplxI_{47–134}$. The P_{vr}, paired-pulse ratio, and Ca^{2+}-sensitivity were only modestly impaired as compared to WT CplxI (Fig. 5c-f). The rescue activity of $CplxI_{26–134}$ L41P was significantly better than that of $CplxI_{27–134}$ ($p < 0.05$ for all of P_{vr}, paired-pulse ratio, and Ca^{2+}-sensitivity; Fig. 5c-f). Collectively, these results demonstrate that the inhibitory function of the accessory α-helix is dependent on the integrity of the α-helical conformation.

Author Manuscript Author Manuscript Author Manuscript Author Manuscript

CplxI N-terminal functions require SNARE complex binding

We next attempted to define the relationship between the SNARE complex binding and the functions of the N-terminal domains of CplxI. Given the WT-like SNARE complex binding of $CplxI_{27–134}$ and its loss-of-function phenotype in rescue experiments, we reasoned that $CplxI_{27–134}$ would be able to compete with WT CplxI for SNARE complex binding and thereby inhibit release in WT neurons. To test this hypothesis, we overexpressed $CplxI_{27–134}$ in WT (or CplxII KO) neurons and compared these to WT (or CplxII KO) neurons overexpressing CplxI WT. We found that overexpression of $CplxI_{27–134}$ resulted in a 32% reduction in P_{vr}, a 32% increase in paired-pulse ratio, and decreased Ca^{2+}-sensitivity (Fig. 6a-d). These data showed that overexpression of $CplxI_{27–134}$ reduced Ca^{2+}-triggered fast neurotransmitter release in WT neurons, but not to the extent observed upon rescue of CplxI/II DKO neurons with $CplxI_{27–134}$ (Fig. 5), most likely because in the former case, the endogenous CplxI still participated in release. Consistent with this idea, overexpression of $CplxI_{27–134}$ in CplxI Het/CplxII KO neurons caused stronger phenotypic changes than in WT neurons (data not shown).

We next introduced the K69A Y70A mutations, which abolish SNARE complex binding (Fig. 3d), into $CplxI_{27–134}$. We found that the K69A Y70A mutations completely prevented the inhibitory effect of $CplxI_{27–134}$ in WT neurons. Overexpression of $CplxI_{27–134}$ K69A Y70A in WT neurons did not alter P_{vr}, paired-pulse ratio, or Ca^{2+}-sensitivity (Fig. 6a-d). Thus, CplxI must first bind to the SNARE complex in order to execute the additional functions through its N-terminal domains (i.e. the first 26 residues and the accessory α-helix). These results also confirmed that $CplxI_{27–134}$ is indeed a loss-of-function mutant and the failure of rescuing CplxI/II-DKO neurons is not a trivial artifact. It is important to note that the sequential actions of the SNARE complex binding region and the N-terminal domains of CplxI could only be revealed by these overexpression experiments in WT neurons, but not by the rescue experiments in CplxI/II DKO neurons, because $CplxI_{27–134}$ and CplxI K69A Y70A behaved similarly in CplxI/II DKO neurons (Figs. 4 and 5).

Both $CplxI_{27–134}$ and CplxI K69A Y70A led to complete loss-of-function phenotypes when expressed in CplxI/II DKO neurons, but the underlying mechanisms are different. The CplxI K69A Y70A phenotype resulted from the loss of CplxI functions altogether, as the functions of the N-terminal domains depend on the SNARE complex interaction. In contrast, the $CplxI_{27–134}$ phenotype is due to the absence of the active function of the first 26 residues, while the remaining positive effect of the central α-helix is counteracted by the inhibitory effect of the accessory α-helix. This notion predicts that removal of the inhibitory function of the accessory α-helix in $CplxI_{27–134}$ will reduce the inhibitory effect of $CplxI_{27–134}$ in WT neurons, similar to the rescue experiments. Indeed, when we overexpressed $CplxI_{41–134}$ or $CplxI_{27–134}$ L41P in WT neurons, we found that $CplxI_{41–134}$ caused little alteration in transmitter release, while $CplxI_{27–134}$ L41P had only a subtle effect (Fig. 6a-d). Together with the results from the rescue experiments, these overexpression studies confirmed that the accessory α-helix inhibits and the first 26 residues facilitate Ca^{2+}-triggered synchronous release.

Author Manuscript Author Manuscript Author Manuscript Author Manuscript

CplxI N terminus facilitates transmitter release in Syt1 KO

The phenotypic similarity between CplxI/II DKO and Syt1 KO indicates that Cplxs and Syt1 may function in the same pathway. We therefore tested the hypothesis that the CplxI N terminus may functionally interact with Syt1 and that the loss-of-function phenotype of $CplxI_{27–134}$ is due to the lack of this functional interaction. If this were the case, $CplxI_{27–134}$ and CplxI WT would behave similarly in the absence of Syt1. Hence, we overexpressed WT CplxI or $CplxI_{27–134}$ in Syt1 KO neurons and compared these to Syt1 KO neurons expressing EGFP only. Typically, neurotransmitter release in hippocampal autaptic neurons can be separated into two components based on their time constants, a fast component with a time constant of 6-7 ms (synchronous release) and a slow component with a time constant of 200-300 ms (asynchronous release)[31,32]. We found that in all of these Syt1 KO neurons, both the time constant and the amplitude of the synchronous release were affected, while the asynchronous release remained (Fig. 7a). When we measured evoked EPSC amplitude, EPSC charge, and P_{vr}, we found no significant changes upon overexpression of WT CplxI in Syt1 KO neurons ($p > 0.05$ for all of three parameters, Fig. 7b-d). However, overexpression of $CplxI_{27–134}$ in Syt1 KO neurons caused substantial reductions in evoked EPSC amplitude, EPSC charge and P_{vr} as compared to Syt1 KO neurons overexpressing WT CplxI or EGFP (Fig. 7b-d). The similar inhibitory effects of $CplxI_{27–134}$ in both WT and Syt1 KO neurons argue against the idea that the loss-of-function phenotype of $CplxI_{27–134}$ is due to the lack of an interaction with Syt1. Rather, these results indicate that the N terminus of CplxI can facilitate Ca^{2+}-triggered neurotransmitter release even in the absence of Syt1. The Ca^{2+}-triggered release in Syt1 KO neurons can still be mathematically separated into two kinetically distinct components, a fast component with a time constant of 30-50 ms and a slow component with a time constant of 300-400 ms (data not shown and refs. 24, 32). When we separated these two release components, we found that overexpression of WT CplxI or $CplxI_{27–134}$ did not change the time constants of the fast and slow components. The reduction of P_{vr} by overexpression of $CplxI_{27–134}$ in Syt1 KO neurons was primarily due to a decrease in the fast component, while the slow component was also slightly reduced (data not shown). Interestingly, the inhibitory effect of $CplxI_{27–134}$ in Syt1 KO neurons seems more pronounced than in WT neurons (Figs. 6a and 7d), suggesting that Syt1 may partially relieves the inhibitory function of the accessory α-helix.

Discussion

Ca^{2+}-triggered neurotransmitter release is the most tightly regulated membrane fusion reaction. It is controlled by a complex protein machinery involving the minimal fusion apparatus and specialized proteins that fine-tune the speed and the Ca^{2+}-sensitity of transmitter release exquisitely. In order to achieve this fast and sophisticated regulation, this machinery is likely suspended in a metastable state that involves a delicate balance between activating and inhibiting interactions. It is biologically feasible that some components of the release machinery may participate in both types of interactions, acting as both activators and inhibitors of release.

Cplxs are key regulators in synaptic exocytosis. Previous studies revealed either a positive[9,16–18] or a negative[19–23] role of Cplxs in exocytosis, based on different

Author Manuscript Author Manuscript Author Manuscript Author Manuscript

manipulations that simply increase or decrease Cplx levels in various systems. In the present study, we dissected the distinct roles of different CplxI domains in controlling Ca^{2+}-triggered fast release. We show that CplxI facilitates transmitter release through its SNARE complex binding region and its first 26 residues, while the accessory α-helix exhibits an inhibitory effect on vesicle fusion. Our data demonstrate the overall positive function of Cplxs in promoting transmitter release and emphasize a dual role for Cplxs in fine-tuning the release process. These results reveal a structural basis to account for both the facilitating and inhibitory functions of Cplxs in Ca^{2+}-triggered release, and lead us to propose a model for the molecular mechanisms of Cplxs function that differ from previous models[12,16,21–23] in several aspects (Fig. 8).

Role of Cplxs binding to the SNARE complex

Our studies of the SNARE complex binding deficient CplxI mutants provide the missing link between the *in vitro* Cplx-SNARE complex interaction and the *in vivo* Cplxs function. The clear correlation between SNARE complex binding and CplxI function (Fig. 4) strongly supports the notion that Cplxs promote synaptic vesicle fusion at least in part through their binding to the SNARE complex. Two mechanisms may contribute to the essential role of this binding in CplxI function. First, this interaction stabilizes the interface between Synaptobrevin 2 and Syntaxin 1. This stabilization effect of CplxI has been shown to extend beyond the CplxI binding region and propagate towards the C terminus of the SNARE complex, which led to the hypothesis that CplxI stabilizes the assembled SNARE complex in preparation for fusion[12]. However, this hypothesis remains to be validated. Second, and perhaps more importantly, CplxI binds to the SNARE complex and subsequently recruits other molecular interactions to facilitate the release process. This notion emerges from the critical findings that CplxI promotes fusion through its first 26 residues, which do not contact the SNARE complex, and that this function is dependent on SNARE complex binding (Figs. 5 and 6). In this context, the SNARE complex serves as a scaffold that properly positions the N terminus of CplxI near the fusion pore to stimulate fast release. It is also plausible that CplxI can recruit additional molecular interactions via residues within the SNARE complex binding region that do not contact the SNARE complex. Considering that full assembly of the SNARE complex C terminus is likely to occur during the Ca^{2+}-triggering step[33], we propose that Cplxs can help to assemble the SNARE complex more fully, but they do not complete SNARE complex assembly (Fig. 8, from step 2 to 3).

Inhibitory function of the accessory α-helix of Cplxs

A fusion clamp role for Cplxs has been proposed based on *in vitro* studies of membrane fusion[21,22], but it is clear that Cplxs do not act solely as a fusion clamp in transmitter release. First, deletion of CplxI and II in hippocampal neurons causes a dramatic reduction in Ca^{2+}-triggered synchronous release[16]. This is unlikely due to the presence and “clamp” action of CplxIII because overexpression of CplxIII rescues the CplxI/II DKO phenotype[9]. Second, the fusion clamp hypothesis[21,22] predicts that increasing or decreasing Cplx levels in the absence of Syt1 should inhibit or enhance release, respectively. Instead, we found that overexpression of WT CplxI in either WT or Syt1 KO neurons did not inhibit transmitter release (Figs. 2 and 7). Moreover, deletion of CplxI and II in Syt1 KO neurons further reduced the release as compared to Syt1 KO (M. Xue. and C. Rosenmund, unpublished

Author Manuscript Author Manuscript Author Manuscript Author Manuscript

results). Third, although overexpression of $CplxI_{27–134}$ in WT neurons led to a reduction in release (Fig. 6), we do not consider $CplxI^{27-134}$ as a fusion clamp. Rather, we interpret $CplxI_{27–134}$ as a loss-of-function mutant lacking the facilitating function of the first 26 residues because overexpression of $CplxI_{27–134}$ in CplxI/II DKO neurons did not further reduce release as compared to CplxI/II DKO neurons (Fig. 5). Nevertheless, the inhibition of fusion by Cplxs in the *in vitro* assays may reflect the negative regulatory role of the accessory α-helix that we identified here. Our results indicate that the inhibitory function of the accessory α-helix of CplxI depends on its helical conformation (Figs. 5 and 6). The crystal structure of the CplxI-SNARE complex shows that the accessory α-helix of CplxI is located right above the C-terminal portion of the Synaptobrevin 2 SNARE motif[12]. Hence, we speculate that the accessory α-helix can replace the C-terminal portion of the Synaptobrevin 2 SNARE motif in the four-helix bundle, and, together with the repulsion between synaptic vesicle and plasma membrane, can prevent the complete assembly of the SNARE complex before the Ca^{2+} influx (Fig. 8, step 3).

Facilitating function of Cplxs in the absence of Syt1

It has been proposed that binding of Cplxs to the SNARE complex stabilizes primed vesicles in a metastable state and that Syt1 acts on this fusion intermediate to trigger synchronous release[12,23,26]. This model implies that Cplxs function upstream of Syt1. However, we identified the first 26 residues of CplxI as a novel facilitator of Ca^{2+}-triggered fast release that can act in the absence of Syt1 (Fig. 7). The mechanistic nature of this process is currently unknown. The first 26 residues may interact with other proteins, CplxI itself or even lipids. For instance, an intramolecular interaction of the first 26 residues with the accessory α-helix and/or the central α-helix could help to relieve the inhibitory effect of the accessory α-helix. However, yeast two hybrid screens and affinity purification experiments so far failed to identify a specific protein interactor (K. Reim and N. Brose, unpublished results). It is also plausible that this very N terminus of CplxI interacts with phospholipid membrane and contributes to the stabilization of the stalk or the perturbation of the bent membrane at the contact site between vesicle and plasma membrane. Currently, it is also unclear whether the positive function of the first 26 residues may be coupled to Syt1 in WT synapses, but works in conjunction with other Ca^{2+} sensors in the absence of Syt1. This facilitating function of the first 26 residues does not involve SNARE complex binding and can be independent of Syt1 (Fig. 8, steps 3 and 4). Therefore, it is possible that the *in vitro* fusion assays using SNAREs and Syt1 would only uncover the inhibitory role of Cplxs[21,22] because the facilitating interaction via the N terminus of Cplxs may be missing in these reductionist systems.

In addition to shedding light on the molecular mechanisms of Cplxs function, our study also supports the notion that the SNARE complex is essential for Ca^{2+}-triggered fast transmitter release. Numerous genetic and biochemical studies demonstrated the essential roles of individual SNARE proteins in synaptic vesicle fusion[1]. It has been proposed that the assembly of the SNARE complex drives membrane fusion[34,35], but *in vivo* evidence for the involvement of the SNARE complex in transmitter release is limited[33,36,37]. We demonstrate here that binding of CplxI to its receptor, the assembled SNARE complex, is crucial for fast transmitter release, thus providing *in vivo* evidence for the importance of the SNARE

Author Manuscript Author Manuscript Author Manuscript Author Manuscript

complex in vesicle fusion. Furthermore, the SNARE complex bound CplxI does not only modulate the complex but apparently also recruits additional interactions. This implies that in addition to its key role in fusion, the SNARE complex functions as a scaffolding platform to recruit other players into the release apparatus.

Methods

Random mutagenesis and cosedimentation assays

Random mutagenesis experiments were performed according to the published procedures[30], either with limiting amounts of dGTP (20 μM), or with limiting amounts of dGTP (20 μM) and an excess of dITP (200 μM). PCR reactions were performed using specific rat CplxI primers with engineered BamHI or EcoRI sites. PCR fragments were subcloned into pCR2.1-TOPO (Invitrogen), sequenced to identify mutations, and then subcloned into pGEX-KG[38]. The resulting vectors expressed WT or mutant CplxI in frame with GST in *E. coli*. Recombinant GST-CplxI fusion proteins were immobilized and purified on glutathione-agarose (Sigma), and used for cosedimentation assays as described[9]. The procedues are described in detail in the Supplementary Data online.

SFV constructs and production

Rat WT and mutant CplxI variants were cloned into a bicistronic SFV expression vector (based on pSFV1; Invitrogen) that contains the respective CplxI cDNA, followed by a papillomavirus IRES, and the EGFP cDNA (from pEGFP-N1; Clontech). Myc-tagged CplxI variants were generated by fusing a linker (SGGSGGTGG) followed by a c-Myc (EQKLISEEDL) to the C terminus of CplxI variants. The generated constructs co-express the respective CplxI variants with EGFP in the same cell, which allows the identification of infected neurons. Virus particle production, activation and infection were performed according to the published protocols27.

Animals and neuronal culture

CplxI/II DKO mice were obtained by interbreeding of mice homozygous for the CplxII mutation and heterozygous for the CplxI mutation as described16. All procedures to maintain and use these mice were approved by the Institutional Animal Care and Use Committee for Baylor College of Medicine and Affiliates, and by the local government agency for the Max Planck Institute of Experimental Medicine. For electrophysiology experiments, collagen/poly-D-lysine microislands were made with a custom-built stamp to achieve uniform size (~200 μm diameter). Astrocytes were grown on microislands for one week before plating neurons. Primary hippocampal neurons were prepared from postnatal day 0 mice, plated at 300 cm-2 density and grown in a chemically defined medium (Neurobasal-A medium supplemented with Glutamax and B-27; Invitrogen). Under these conditions, a single neuron on the astrocyte microisland forms recurrent synapses (autapses)39. For Western blotting and immunocytochemistry of protein expression, neurons were plated at 10,000 cm-2 and 5,000 cm-2 densities on continental astrocyte feeder layer, respectively.

Author Manuscript Author Manuscript Author Manuscript Author Manuscript

Western blotting and immunocytochemistry

Proteins were extracted 10-11 hours after neurons were infected with SFV. Expression levels of WT and mutant CplxI variants were estimated by Western blotting. Neurons were fixed with 4% (w/v) paraformaldehyde 10 hours after SFV infection. The presynaptic targeting of WT and mutant CplxI variants were examined by immunocytochemistry and confocal microscopy. The procedues are described in detail in the Supplementary Data online.

Electrophysiology of autaptic hippocampal neurons

In each experiment, approximately equal numbers of neurons from every group were measured in parallel on the same day in vitro (9-14 DIV). Only the microislands containing a single neuron were used for experiments. Whole-cell voltage-clamp recordings were performed between 9 hours and 12 hours after neurons were infected with SFV. The neurons were clamped at –70 mV with an Axopatch 200B amplifier (Molecular Devices, Inc.) under the control of Clampex 9.2 or 10.0 (Molecular Devices, Inc.). The data were acquired at 10 kHz and low-pass filtered at 5 kHz. The series resistance was compensated about 80% and only cells with series resistances below 10 MΩ were analyzed. The patch pipette solution contained (mM): K-Gluconate, 146; HEPES, 17.8; EGTA, 1; MgCl2, 0.6; ATP-Mg, 4; GTP-Na, 0.3; Phosphocreatine, 12 and Phosphocreatine kinase 50U ml-1. The standard extracellular solution contained (mM): NaCl, 140; KCl, 2.4; HEPES, 10; glucose, 10; CaCl2, 4; MgCl2, 4; 300 mOsm, pH 7.4. For Ca2+-sensitivity experiments, Mg2+ concentration was kept at 1 mM and Ca2+ concentration varied as indicated. Hypertonic solution for measuring RRP size was made by adding 500 mM sucrose to the standard extracellular solution28. Fast solution exchange was archived with a microperfusion device (SF-77B, Warner Instruments, Inc.).

Action potential evoked EPSC was triggered by a 2 ms somatic depolarization to 0 mV. Neurons were stimulated at 0.2 Hz in standard extracellular solution to measure basal EPSCs. RRP size was determined by measuring the charge transfer of the transient synaptic current induced by a pulsed 4 s-long application of hypertonic sucrose solution directly onto the neuron. To obtain vesicular release probability (P_{vr}), the evoked EPSC and the response to the hypertonic sucrose solution were recorded successively from the same neuron. Evoked EPSC was integrated for 1 s to calculate the charge transfer. P_{vr} was calculated by the ratio of evoked EPSC charge and RRP size. Short-term plasticity was examined by evoking 5 EPSCs at 50 Hz in standard extracellular solution, and paired-pulse ratio was measured by dividing the second EPSC amplitude with the first EPSC amplitude. To examine the apparent Ca^{2+}-sensitivity of synchronous release, EPSCs were evoked at 0.2 Hz in different Ca^{2+} concentrations (12 mM or 1 mM). Each test measurement was preceded and followed by a measurement in standard extracellular solution to control for the rundown of synaptic responses. The EPSC amplitude in each Ca^{2+} concentration was normalized to the amplitude in standard extracellular solution[16]. All experiments were performed at room temperature (23-24°C). Data were analyzed offline using AxoGraph 4.9 or AxoGraph X 1.0 (AxoGraph Scientific). Statistic significances were tested using Student's test, nonparametric Mann-Whitney test or One-way ANOVA.

Author Manuscript Author Manuscript Author Manuscript Author Manuscript

Supplementary Material

Refer to Web version on PubMed Central for supplementary material.

Acknowledgments

We thank T. Hellmann, I. Herfort, D. Reuter, S. Wenger, A. Zeuch (all Göttingen, Germany), H. Chen (Houston, USA) for excellent technical assistance, and F. Benseler, D. Schwerdtfeger, and I. Thanhäuser (all Göttingen, Germany) for DNA sequencing and oligonucelotide synthesis. We thank R. Nehring and R. Atkinson for technical advice. We are grateful to H. Bellen for comments on the manuscript, and E. Neher for continuous support and advice. This work was supported by the Deutsche Forschungsgemeinschaft (SFB 523/B9 to N.B. and C.R.), by a Heisenberg Fellowship (to C.R.), by the Brown Foundation (to C.R.), by the NIH (NS50655 to C.R., NS37200 to J.R.), and by Baylor Research Advocates for Student Scientists and a McNair Fellowship (both to H.T.C.).

References

1. Jahn R, Scheller RH. SNAREs - engines for membrane fusion. Nat Rev Mol Cell Biol. 2006; 7:631–43. [PubMed: 16912714]
2. Antonin W, Fasshauer D, Becker S, Jahn R, Schneider TR. Crystal structure of the endosomal SNARE complex reveals common structural principles of all SNAREs. Nat Struct Biol. 2002; 9:107–11. [PubMed: 11786915]
3. Sutton RB, Fasshauer D, Jahn R, Brunger AT. Crystal structure of a SNARE complex involved in synaptic exocytosis at 2.4 A resolution. Nature. 1998; 395:347–53. [PubMed: 9759724]
4. Rizo J, Chen X, Arac D. Unraveling the mechanisms of synaptotagmin and SNARE function in neurotransmitter release. Trends Cell Biol. 2006; 16:339–50. [PubMed: 16698267]
5. Fernandez-Chacon R, et al. Synaptotagmin I functions as a calcium regulator of release probability. Nature. 2001; 410:41–9. [PubMed: 11242035]
6. Ishizuka T, Saisu H, Odani S, Abe T. Synaphin: a protein associated with the docking/fusion complex in presynaptic terminals. Biochem Biophys Res Commun. 1995; 213:1107–14. [PubMed: 7654227]
7. Takahashi S, et al. Identification of two highly homologous presynaptic proteins distinctly localized at the dendritic and somatic synapses. FEBS Lett. 1995; 368:455–60. [PubMed: 7635198]
8. McMahon HT, Missler M, Li C, Sudhof TC. Complexins: cytosolic proteins that regulate SNAP receptor function. Cell. 1995; 83:111–9. [PubMed: 7553862]
9. Reim K, et al. Structurally and functionally unique complexins at retinal ribbon synapses. J Cell Biol. 2005; 169:669–80. [PubMed: 15911881]
10. Pabst S, et al. Rapid and selective binding to the synaptic SNARE complex suggests a modulatory role of complexins in neuroexocytosis. J Biol Chem. 2002; 277:7838–48. [PubMed: 11751907]
11. Pabst S, et al. Selective interaction of complexin with the neuronal SNARE complex. Determination of the binding regions. J Biol Chem. 2000; 275:19808–18. [PubMed: 10777504]
12. Chen X, et al. Three-dimensional structure of the complexin/SNARE complex. Neuron. 2002; 33:397–409. [PubMed: 11832227]
13. Bracher A, Kadlec J, Betz H, Weissenhorn W. X-ray structure of a neuronal complexin-SNARE complex from squid. J Biol Chem. 2002; 277:26517–23. [PubMed: 12004067]
14. Hu K, Carroll J, Rickman C, Davletov B. Action of complexin on SNARE complex. J Biol Chem. 2002; 277:41652–6. [PubMed: 12200427]
15. Bowen ME, Weninger K, Ernst J, Chu S, Brunger TA, Single Molecule. Studies of Synaptotagmin and Complexin Binding to the SNARE Complex. Biophys J. 2005
16. Reim K, et al. Complexins regulate a late step in Ca2+-dependent neurotransmitter release. Cell. 2001; 104:71–81. [PubMed: 11163241]
17. Tokumaru H, et al. SNARE complex oligomerization by synaphin/complexin is essential for synaptic vesicle exocytosis. Cell. 2001; 104:421–32. [PubMed: 11239399]

Author Manuscript Author Manuscript Author Manuscript Author Manuscript

18. Tadokoro S, Nakanishi M, Hirashima N. Complexin II facilitates exocytotic release in mast cells by enhancing Ca2+ sensitivity of the fusion process. J Cell Sci. 2005; 118:2239–46. [PubMed: 15870114]
19. Itakura M, Misawa H, Sekiguchi M, Takahashi S, Takahashi M. Transfection analysis of functional roles of complexin I and II in the exocytosis of two different types of secretory vesicles. Biochem Biophys Res Commun. 1999; 265:691–6. [PubMed: 10600482]
20. Ono S, et al. Regulatory roles of complexins in neurotransmitter release from mature presynaptic nerve terminals. Eur J Neurosci. 1998; 10:2143–52. [PubMed: 9753100]
21. Giraudo CG, Eng WS, Melia TJ, Rothman JE. A clamping mechanism involved in SNARE-dependent exocytosis. Science. 2006; 313:676–80. [PubMed: 16794037]
22. Schaub JR, Lu X, Doneske B, Shin YK, McNew JA. Hemifusion arrest by complexin is relieved by Ca(2+)-synaptotagmin I. Nat Struct Mol Biol. 2006; 13:748–50. [PubMed: 16845390]
23. Tang J, et al. A complexin/synaptotagmin 1 switch controls fast synaptic vesicle exocytosis. Cell. 2006; 126:1175–87. [PubMed: 16990140]
24. Geppert M, et al. Synaptotagmin I: a major Ca2+ sensor for transmitter release at a central synapse. Cell. 1994; 79:717–727. [PubMed: 7954835]
25. Yoshihara M, Littleton JT. Synaptotagmin I functions as a calcium sensor to synchronize neurotransmitter release. Neuron. 2002; 36:897–908. [PubMed: 12467593]
26. Sudhof TC. The synaptic vesicle cycle. Annu Rev Neurosci. 2004; 27:509–47. [PubMed: 15217342]
27. Ashery U, Betz A, Xu T, Brose N, Rettig J. An efficient method for infection of adrenal chromaffin cells using the Semliki Forest virus gene expression system. Eur J Cell Biol. 1999; 78:525–532. [PubMed: 10494858]
28. Rosenmund C, Stevens CF. Definition of the readily releasable pool of vesicles at hippocampal synapses. Neuron. 1996; 16:1197–207. [PubMed: 8663996]
29. Morton AJ, Edwardson JM. Progressive depletion of complexin II in a transgenic mouse model of Huntington's disease. J Neurochem. 2001; 76:166–72. [PubMed: 11145989]
30. Spee JH, de Vos WM, Kuipers OP. Efficient random mutagenesis method with adjustable mutation frequency by use of PCR and dITP. Nucleic Acids Res. 1993; 21:777–8. [PubMed: 8441702]
31. Goda Y, Stevens CF. Two components of transmitter release at a central synapse. Proc Natl Acad Sci U S A. 1994; 91:12942–6. [PubMed: 7809151]
32. Shin OH, et al. Sr2+ binding to the Ca2+ binding site of the synaptotagmin 1 C2B domain triggers fast exocytosis without stimulating SNARE interactions. Neuron. 2003; 37:99–108. [PubMed: 12526776]
33. Sorensen JB, et al. Sequential N- to C-terminal SNARE complex assembly drives priming and fusion of secretory vesicles. Embo J. 2006; 25:955–66. [PubMed: 16498411]
34. Lin RC, Scheller RH. Structural organization of the synaptic exocytosis core complex. Neuron. 1997; 19:1087–94. [PubMed: 9390521]
35. Hanson PI, Roth R, Morisaki H, Jahn R, Heuser JE. Structure and conformational changes in NSF and its membrane receptor complexes visualized by quick-freeze/deep-etch electron microscopy. Cell. 1997; 90:523–35. [PubMed: 9267032]
36. Xu T, et al. Inhibition of SNARE complex assembly differentially affects kinetic components of exocytosis. Cell. 1999; 99:713–22. [PubMed: 10619425]
37. Littleton JT, et al. Temperature-sensitive paralytic mutations demonstrate that synaptic exocytosis requires SNARE complex assembly and disassembly. Neuron. 1998; 21:401–13. [PubMed: 9728921]
38. Guan KL, Dixon JE. Eukaryotic proteins expressed in Escherichia coli: an improved thrombin cleavage and purification procedure of fusion proteins with glutathione S-transferase. Anal Biochem. 1991; 192:262–7. [PubMed: 1852137]
39. Bekkers JM, Stevens CF. Excitatory and inhibitory autaptic currents in isolated hippocampal neurons maintained in cell culture. Proc Natl Acad Sci U S A. 1991; 88:7834–8. [PubMed: 1679238]

Author Manuscript Author Manuscript Author Manuscript Author Manuscript

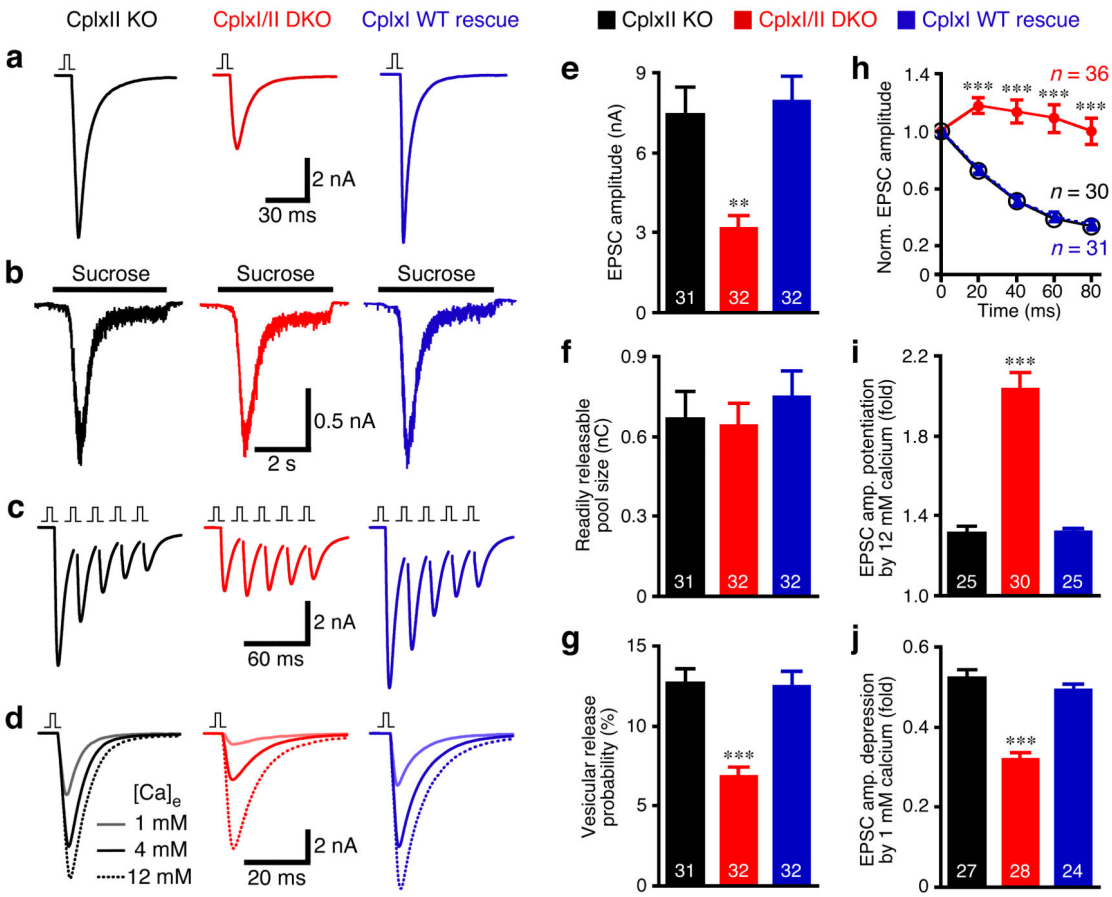

Figure 1. Overexpression of CplxI rescues CplxI/II DKO neurons

CplxI/II DKO neurons overexpressing either EGFP or CplxI WT-IRES-EGFP were compared to CplxII KO neurons overexpressing EGFP.

(**a-c**) Representative traces of basal evoked EPSCs (**a**), synaptic responses to hypertonic sucrose solution (**b**) and 5 EPSCs evoked at 50 Hz (**c**). The vertical bar represents a 2 ms somatic depolarization and the depolarization artifact is blanked.

(**d**) Representative Ca^{2+}-sensitivity experiments in which EPSCs were evoked in standard extracellular solution (4 mM Ca^{2+}/4 mM Mg^{2+}) and in solutions containing 12 mM Ca^{2+}/1 mM Mg^{2+} or 1 mM Ca^{2+}/1 mM Mg^{2+}.

(**e-j**) Summary data of the synaptic properties. Bar graphs show EPSC amplitude (**e**), RRP size (**f**), and vesicular release probability (P_{vr}) (**g**). The amplitudes of 5 EPSCs evoked at 50 Hz were normalized to the first EPSC amplitude and plotted over time (**h**). Bar graphs show EPSC amplitude potentiation (**i**) or depression (**j**) by elevating or lowering Ca^{2+} concentration, respectively. Data are expressed as mean ± SEM. Analyzed neuron numbers are indicated on the bars; ** indicates $p < 0.001$, *** indicates $p < 0.0001$ as compared to CplxII KO neurons.

Author Manuscript Author Manuscript Author Manuscript Author Manuscript

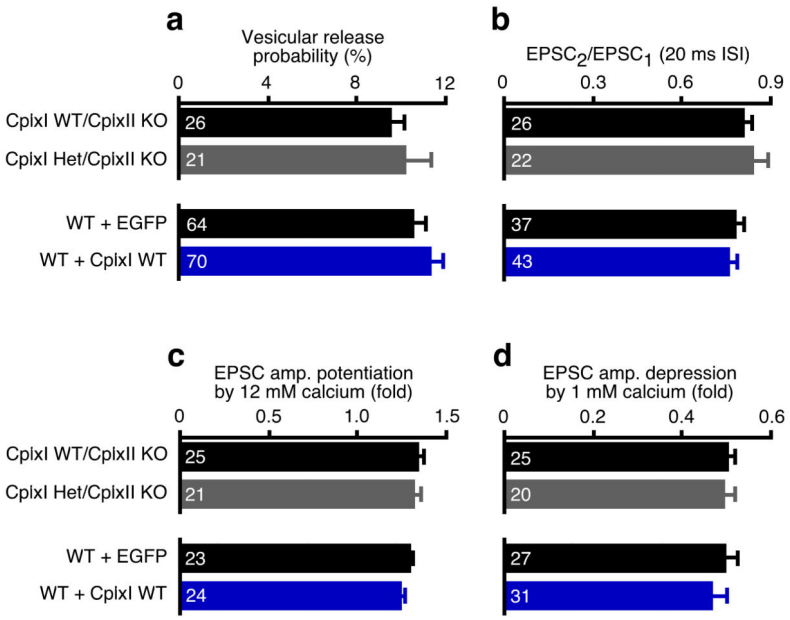

Figure 2. Synaptic function is not sensitive to Cplx levels

CplxI Het/CplxII KO neurons were compared to CplxII KO neurons. WT neurons overexpressing CplxI WT-IRES-EGFP were compared to those overexpressing EGFP. Bar graphs show P_{vr} (**a**), paired-pulse ratio at 20 ms inter-stimulus interval (ISI) (**b**), and EPSC amplitude potentiation (**c**) or depression (**d**) by elevating or lowering Ca^{2+} concentration, respectively. Data are expressed as mean ± SEM. Analyzed neuron numbers are indicated on the bars.

Author Manuscript Author Manuscript Author Manuscript Author Manuscript

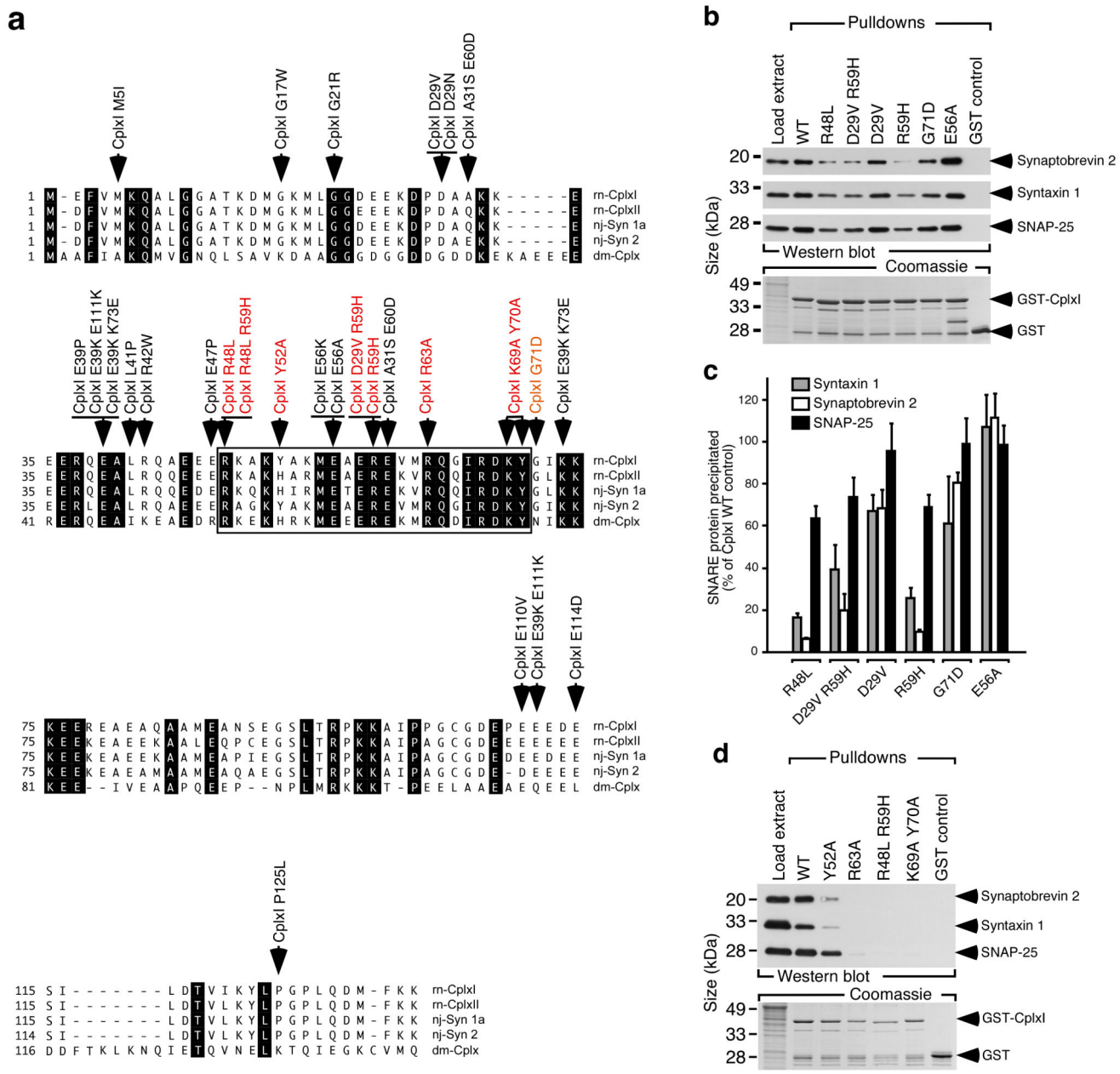

Figure 3. Identification of mutations in CplxI that block SNARE complex binding

(**a**) The amino acid sequences of *Rattus norvegicus* (rn) CplxI and II, *Narke japonica* (nj) Synaphin 1a (Syn 1a) and Synaphin 2 (Syn 2), and *Drosophila melanogaster* (dm) Cplx are shown in single letter amino acid code and aligned for maximal homology. GenBank accession numbers are: NM_022864, rn CplxI; NM_053878, rn CplxII; AB004243, nj Syn 1a; AB004245, nj Syn 2; AY121629, dm Cplx. Identical residues are shown on black background. The boxed region indicates the SNARE complex binding region defined in rn CplxI (aa 48-70). Arrows indicate the single and double amino acid changes generated by mutagenesis (colored: mutations that cause changes in SNARE complex binding).

Author Manuscript Author Manuscript Author Manuscript Author Manuscript

(**b**) Representative cosedimentation assays of WT GST-CplxI, mutant GST-CplxI (R48L, D29V R59H, D29V, R59H, G71D, E56A) fusion proteins and GST alone. Note that R48L, R59H, D29V R59H, and G71D showed reduced SNARE complex binding.
(**c**) Quantification of precipitated SNARE complex components by CplxI variants. Note that Synaptobrevin 2 and Syntaxin 1 were more strongly affected than SNAP-25 by the binding deficient CplxI mutants, indicating that under our experimental conditions CplxI binds to both trimeric SNARE complex and Synaptobrevin 2-Syntaxin 1 dimer. Data are expressed as mean ± SEM (n = 3).
(**d**) Representative cosedimentation assays of WT GST-CplxI, mutant GST-CplxI (Y52A, R63A, R48L R59H, K69A Y70A) fusion proteins and GST alone (n=3). Note that Y52A showed a strong reduction of binding to the SNARE complex, whereas the SNARE complex bindings of R63A, R48L R59H and K69A Y70A were abolished.

Author Manuscript Author Manuscript Author Manuscript Author Manuscript

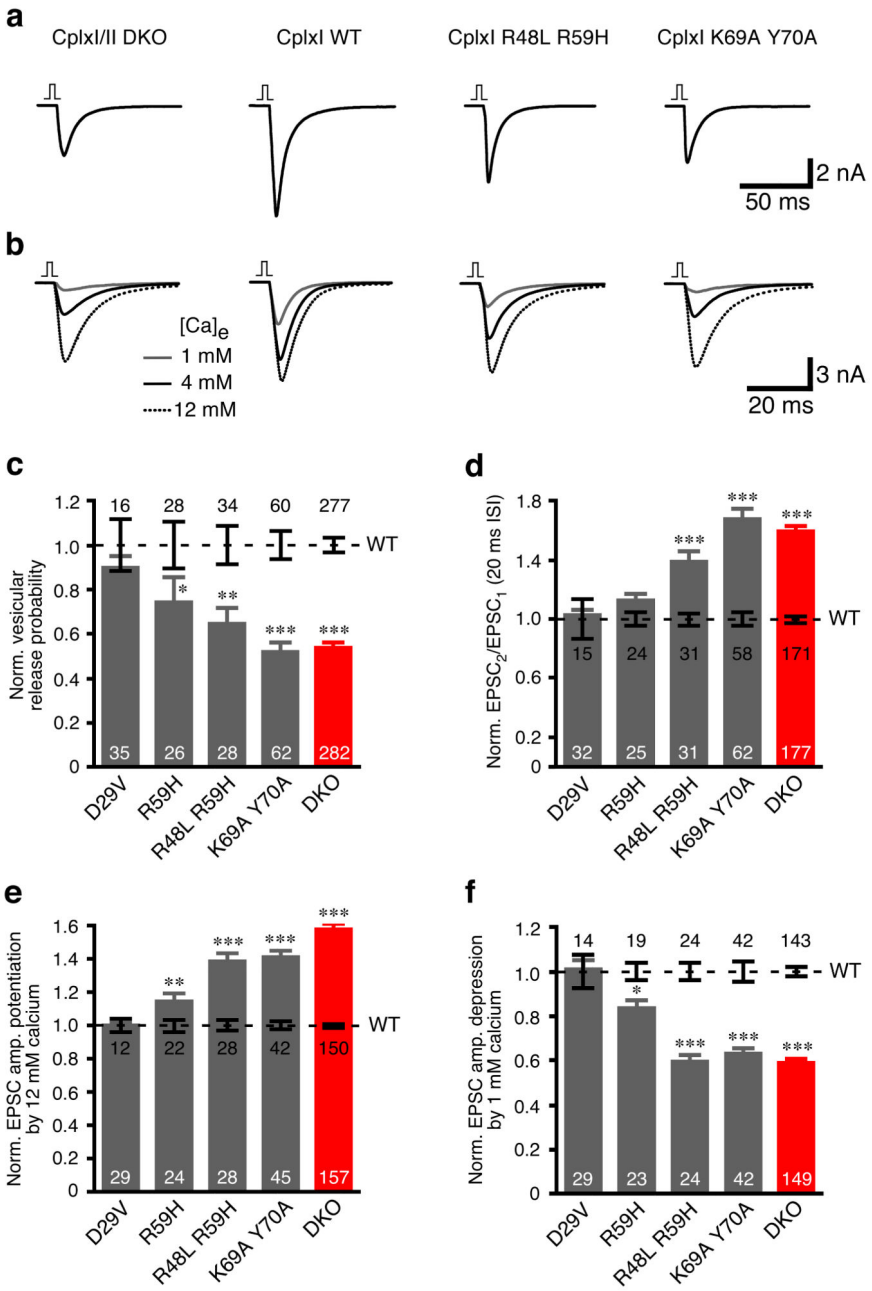

Figure 4. Rescue of CplxI/II DKO neurons with SNARE complex binding deficient CplxI mutants

(**a-b**) Representative traces of basal evoked EPSCs (**a**) and evoked EPSCs in Ca^{2+}-sensitivity experiments (**b**). The vertical bar represents a 2 ms somatic depolarization and the depolarization artifact is blanked.

(**c-f**) Summary data of CplxI/II DKO neurons rescued with CplxI WT-IRES-EGFP (control) or CplxI mutant-IRES-EGFP. Data were normalized to the mean values of the respective controls (dotted line). Bar graphs show P_{vr} (**c**), paired-pulse ratio (**d**), and EPSC amplitude potentiation (**e**) or depression (**f**) by elevating or lowering Ca^{2+} concentration, respectively. Data are expressed as mean ± SEM. Analyzed neuron numbers are indicated on the bars; *

indicates $p < 0.05$, ** indicates $p < 0.01$, *** indicates $p < 0.0001$ as compared to corresponding CplxI WT rescue.

Author Manuscript Author Manuscript Author Manuscript Author Manuscript

Author Manuscript Author Manuscript Author Manuscript Author Manuscript

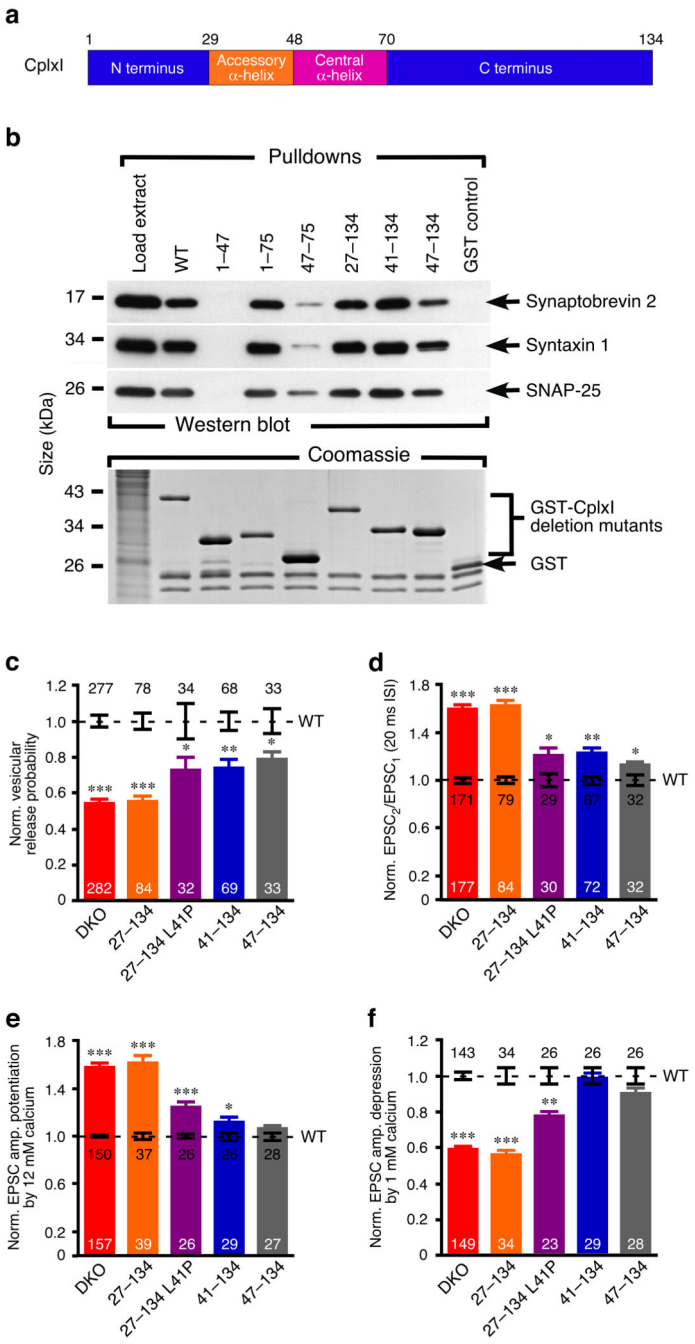

Figure 5. SNARE complex bindings and functions of CplxI N-terminal mutants

(**a**) Schematic diagram of the domain organization of CplxI.

(**b**) Representative cosedimentation assays of WT GST-CplxI, mutant GST-CplxI (1–47, 1–75, 47–75, 27–134, 41–134, 47–134) fusion proteins and GST alone (n=2). $CplxI_{1–47}$ did not bind to the SNARE complex, whereas the SNARE complex bindings of $CplxI_{1–75}$, $CplxI_{27–134}$, and $CplxI_{41–134}$ were normal. Note that $CplxI_{47–75}$ showed drastic reduced binding to the SNARE complex, while $CplxI_{47–134}$ only exhibited slight decreased SNARE complex binding.

Author Manuscript Author Manuscript Author Manuscript Author Manuscript

(**c-f**) Summary data of CplxI/II DKO neurons rescued with CplxI WT-IRES-EGFP (control) or CplxI mutant-IRES-EGFP. Data were normalized to the mean values of the respective controls (dotted line). Bar graphs show P_{vr} (**c**), paired-pulse ratio (**d**), and EPSC amplitude potentiation (**e**) or depression (**f**) by elevating or lowering Ca^{2+} concentration, respectively. Data are expressed as mean ± SEM. Analyzed neuron numbers are indicated on the bars; * indicates $p < 0.05$, ** indicates $p < 0.001$, *** indicates $p < 0.0001$ as compared to corresponding CplxI WT rescue.

Author Manuscript Author Manuscript Author Manuscript Author Manuscript

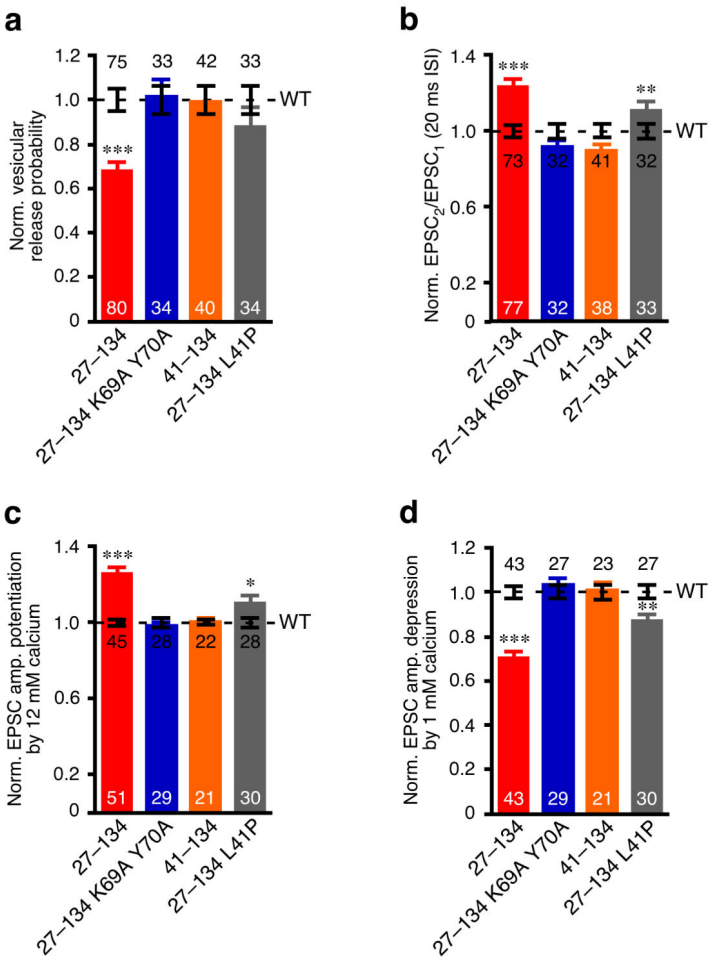

Figure 6. Overexpression of CplxI N-terminal mutants in WT neurons

Summary data of WT neurons overexpressing CplxI WT-IRES-EGFP (control) or CplxI mutant-IRES-EGFP. Data were normalized to the mean values of the respective controls (dotted line). Bar graphs show P_{vr} (**a**), paired-pulse ratio (**b**), and (**c-d**) EPSC amplitude potentiation (**c**) or depression (**d**) by elevating or lowering Ca^{2+} concentration, respectively. Data are expressed as mean ± SEM. Analyzed neuron numbers are indicated on the bars; * indicates $p < 0.05$, ** indicates $p < 0.01$, *** indicates $p < 0.0001$ as compared to overexpression of CplxI WT.

Author Manuscript Author Manuscript Author Manuscript Author Manuscript

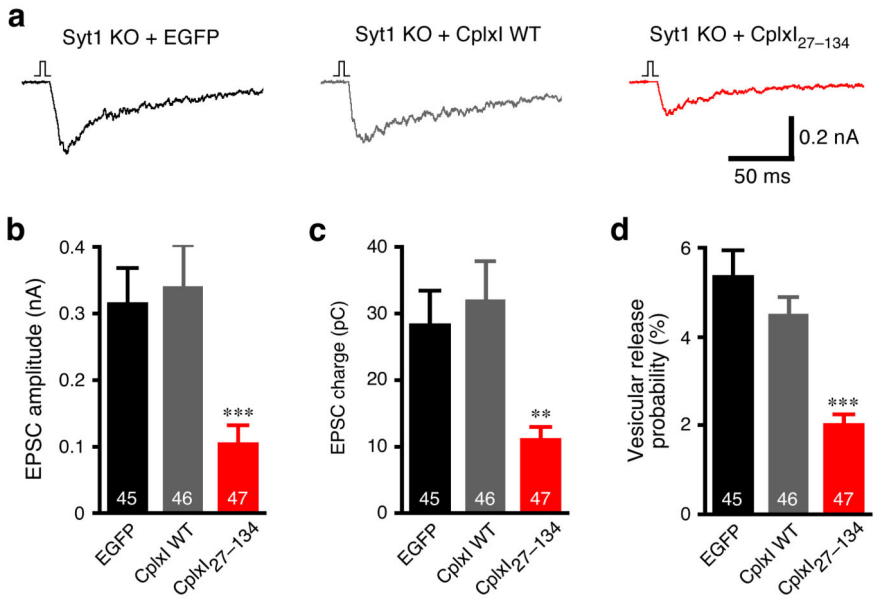

Figure 7. Overexpression of CplxI WT and CplxI$_{27–134}$ in Syt1 KO neurons

(**a**) Representative traces of basal evoked EPSCs of Syt1 KO neurons overexpressing EGFP, CplxI WT-IRES-EGFP or CplxI$_{27–134}$-IRES-EGFP. The vertical bar represents a 2 ms somatic depolarization and the depolarization artifact is blanked.

(**b-d**) Bar graphs show summary data of EPSC amplitude (**b**), EPSC charge (**c**) and P_{vr} (**d**). Data are expressed as mean ± SEM. Analyzed neuron numbers are indicated on the bars; ** indicates $p < 0.001$, *** indicates $p < 0.0001$ as compared to Syt1 KO neurons overexpressing EGFP alone or CplxI WT.

Author Manuscript Author Manuscript Author Manuscript Author Manuscript

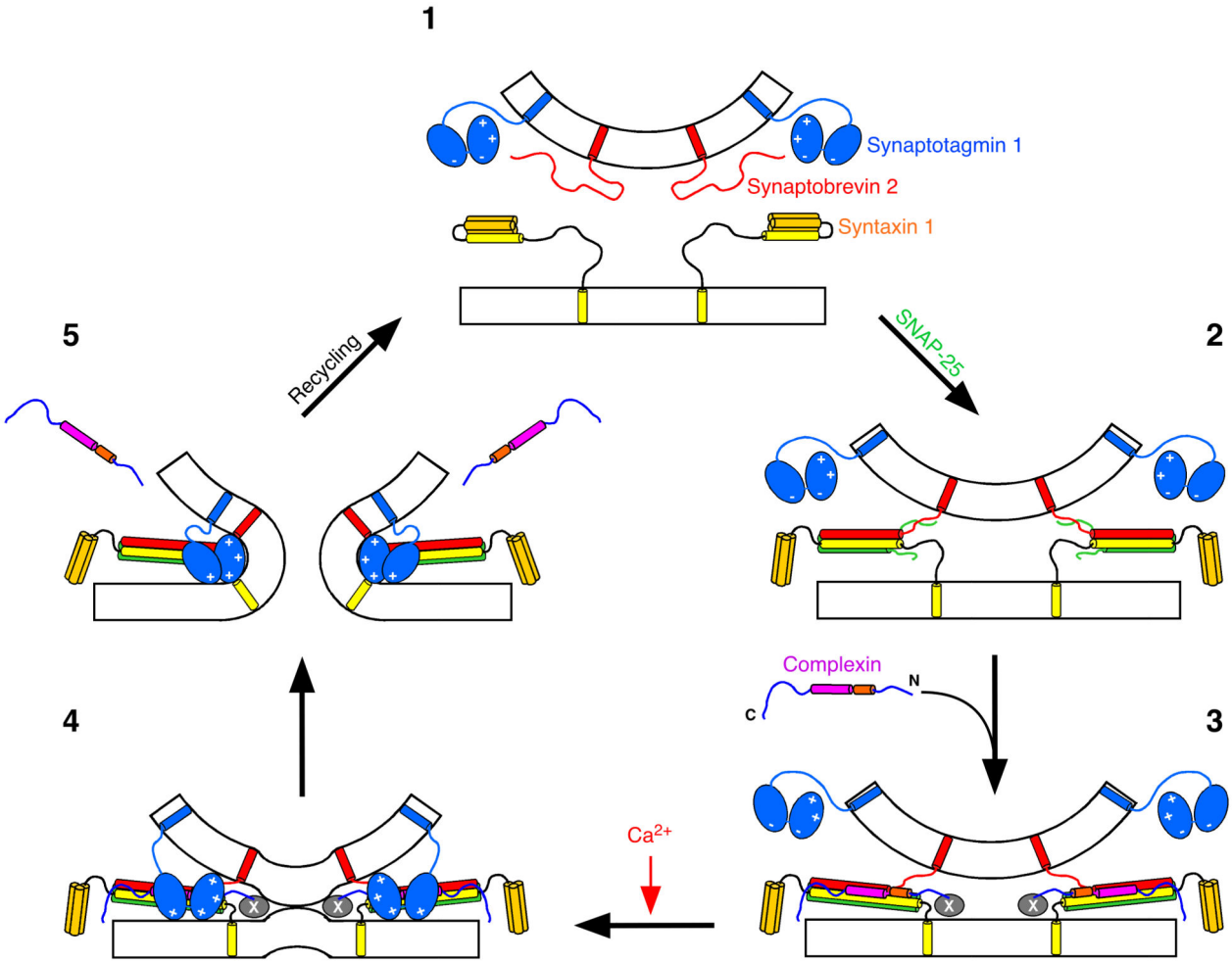

Figure 8. Model for Cplxs function in Ca^{2+}-triggered neurotransmitter release

During priming (the transition from step **1** to **2**), the SNARE complex forms in the N to C terminus direction. However, the "zippering" process is not complete at this stage and the C terminus of the SNARE complex is still partially unstructured. Cplxs bind to this partly assembled SNARE complex through its central α-helix (Step **3**). The binding of Cplxs helps to stabilize the SNARE complex, which could in part contribute to the positive function of Cplxs. At the same time, the accessory α-helix occupies the position of the C-terminal portion of the Synaptobrevin 2 SNARE motif and thereby hinders the full assembly of the SNARE complex before the Ca^{2+} influx (Step **3**). Meanwhile, SNARE complex binding of Cplxs positions the N terminus of Cplxs near the fusion pore to recruit other unknown interactions (the factor(s) X) that facilitate vesicle fusion (Step **3**). Following the Ca^{2+} influx, Ca^{2+} bound Syt1 interacts with the phospholipid membrane and the SNARE complex, and fully assembles the SNARE complex (step **4**), resulting in fusion-pore opening (step **5**). During this process, Cplxs are displaced from the SNARE complex.